

2018 SUMMER STUDENTS ITALIAN PROGRAM AT THE FERMI
NATIONAL ACCELERATOR LABORATORY AND AT OTHER US
LABORATORIES

Study of the Radiative Muon Capture background in the Mu2e experiment

Author
LORENZO PICA

Supervisor
ROBERT H. BERNSTEIN

October 22, 2018

Abstract:

This document presents a study about the Radiative Muon Capture process, in particular spectra for e^\pm created by the conversion of emitted photons. The study was performed because the process can be a non-negligible background in e^\pm momentum spectrum in the Mu2e experiment. Simulations were performed using the theoretical description and previous measurements. Momentum spectra extracted from simulations have been compared with each other and also with Decay In Orbit background. Spectra are dependent by the maximum momentum of emitted photons. It was seen that the contribution to e^- spectrum of Radiative Muon Capture process is non-negligible compared to Decay In Orbit process.

Contents

1	Introduction	2
2	The Mu2e experiment	2
2.1	Experimental overview	2
2.2	Signal	5
2.3	Backgrounds	5
2.4	Lepton Number Violation search	7
3	Radiative Muon Capture	8
3.1	Theoretical description of RMC	9
3.2	Previous measurements	11
4	Data samples	14
4.1	Normalization of histograms	15
4.2	Spectrum histograms	17
5	Comparison between spectra	18
5.1	e^- spectra comparison	18
5.2	e^+ spectra comparison	20
6	Conclusions	21
7	Next steps	21
8	Appendix	22

1 Introduction

The discovery of neutrino oscillations is proof of the existence of a lepton flavor violating process. Evidence of this kind of flavor violation has become a matter of fact in the neutral sector of leptons, but nothing similar has ever been seen in the charged sector of leptons, despite several experiments performed during the last decades to search for them [1]. In these searches only upper limits on branching ratio of these processes were settled.

A new generation of experiment has been designed, improving technologies and techniques in order to reach limits beyond the current ones.

2 The Mu2e experiment

One of these experiments is Mu2e, located at Fermilab, that searches for muon to electron conversion process $\mu^- N \rightarrow e^- N$. This search is performed measuring the number of conversions occurred, then this is normalized to the total number of captured muons:

$$R_{\mu e} = \frac{\mu^- N \rightarrow e^- N}{\mu^- N \rightarrow \text{all muon captures}}$$

It is planned to reach a single event sensitivity four orders-of-magnitude beyond the current limit on $R_{\mu e}$, hence $3 \cdot 10^{-17}$.

2.1 Experimental overview

An overview of the apparatus is given in Figure 1.

In Mu2e, to detect the conversion of a muon to an electron, interacting with a nucleus, muons are stopped in material (here aluminum) in order to let them fall into a bound state with nuclei, and permit the interaction between the two. Then the momentum and the energy of the outgoing particles are measured, to measure the spectrum of the outgoing electrons and positrons.

To do this a muon beam is required with an intensity high enough to reach the needed statistics. The muon beam is produced using a proton beam (provided by Fermilab accelerators), and a solenoid complex. The proton beam enters the production solenoid and hits the production target (tungsten), yielding many pions; these pions decay into muons. Backwards-going (and part of the forwards-going) muons are collected by the gradient present in the magnetic field of the production solenoid. Then these particles are carried to the stopping target by the s-shaped transport solenoid. With this specific shape positive and

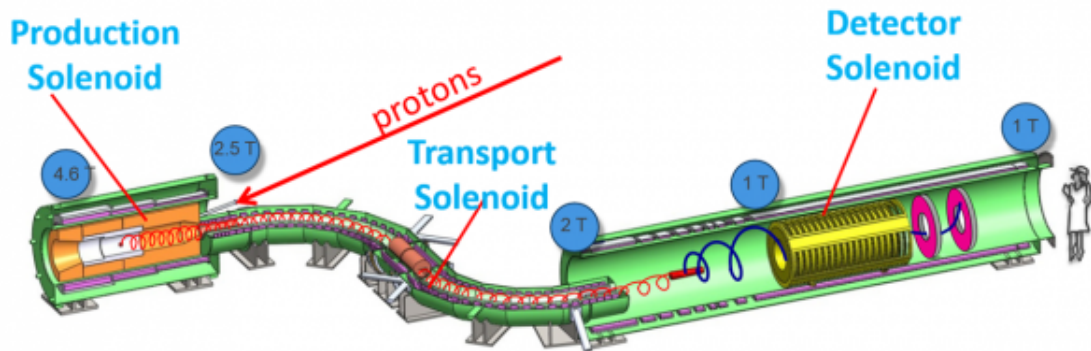


Figure 1: Apparatus of Mu2e experiment.

negative muons drift in opposite directions, so it is possible to select one single particle charge with a collimator, placed in the middle of the transport solenoid. One wants to use only negative muons, the only ones that create bound states with nuclei.

Part of the muon beam stops in the stopping target, creating muonic atoms. From this state some reactions can occur (they will be discussed later) and the outgoing particles are revealed by the detector system.

The detector is composed of a tracker and a calorimeter, both of them with an annular geometry. The tracker is a straw tube tracker, divided in 18 stations, each composed of two plans and each plane of 6 panels. The structure can be seen in Figure 2.

The choice of this technology allows the tracker to have an high resolution, minimizing the energy loss of the particles in material which compose the tracker.

The calorimeter is composed of 674 homogeneous undoped CsI crystals, each of them read out by a SiPM. The calorimeter consists of two disks, at a distance that is the "half-length" of the motion of conversion electron, so if one

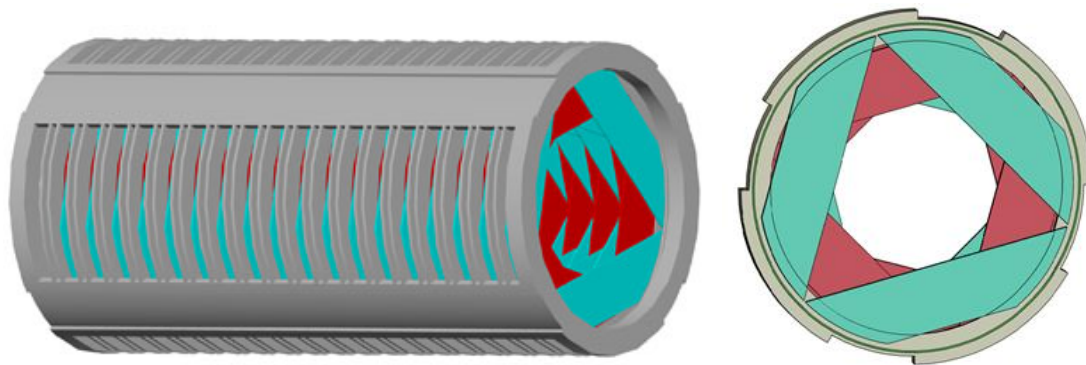


Figure 2: Side (left) and frontal (right) view of the Mu2e tracker.

electron passes through the hole of the first disk, it will hit the second disk. The calorimeter allows the experiment to improve particle identification and tracking, in addition it provides a standalone trigger. The structure of the Mu2e calorimeter can be seen in Figure 3.

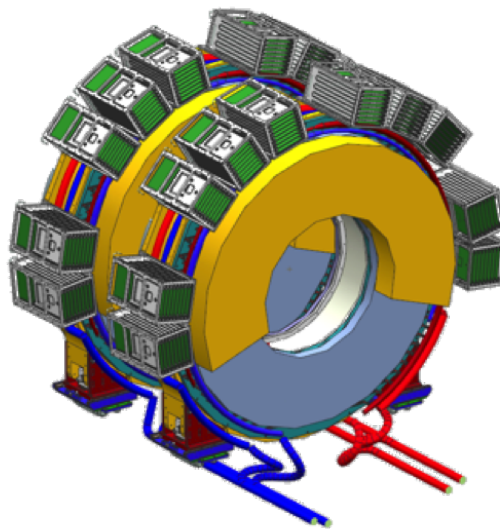


Figure 3: Calorimeter of the Mu2e experiment.

Another essential part of the experiment is the cosmic ray veto. It allows the experiment to recognize fake signals that are caused by cosmic rays. The cosmic ray veto surrounds the detector and the transport solenoid, excepting the face where the transport solenoid passes. It is composed by four layers of scintillators, separated by Al plates; inside the scintillator is present a wavelength-shifting fiber, read out by a SiPM. The veto inefficiency is $< 0.01\%$

and the deadtime is estimated to be $\approx 5\%$.

2.2 Signal

The signal is a detected electron coming from the conversion of a muon. The conversion event has a really specific signature: a single outgoing electron, without the emission of any neutrino, with monochromatic energy. The conversion energy is given by:

$$E_e = m_\mu - B_\mu - E_{N,rec} = 104.973 \text{ MeV}$$

Where m_μ is the muon mass, B_μ is the muonic atom binding energy and $E_{N,rec}$ is the recoil energy of the nucleus.

This kind of signature is a big advantage for the experiment, seen that very few processes produce that kind of signal and the background is very low.

2.3 Backgrounds

The most intense backgrounds have driven the apparatus, detector and beam design, in order to obtain the smallest contribute as possible in terms of number of background events.

Decay In Orbit (DIO) is the most intense intrinsic background. It is defined as intrinsic because it is related to the muons used to measure $R_{\mu e}$. It is due to the β -decay of the muons ($\mu^- \rightarrow e^- \bar{\nu}_e \nu_\mu$), while they are in orbit around the nucleus. The spectrum of usual decay (Michel spectrum) has an endpoint at 52.8 MeV, but it is modified here, because of the interaction that the outgoing electron can have with the nucleus. The energy that the electron can gain in this interaction leads to a spectrum with a long tail, with an endpoint at the conversion energy. DIOs spectrum can be seen in Figure 4.

From this spectrum it is possible to understand why the annular structure for the detector was chosen. With that structure, and the selected radius, only particles with a momentum greater than ~ 80 MeV are detected. This permits to have a huge reduction of event detections, indeed only 10^{-12} of the DIOs reaches the detector.

The structure allows the detector also to not detect muons from the beam that do not stop in the target, and other particles, produced by the interaction of muons with the stopping target, or from interaction of protons with the production target, carried to the detection system like muons.

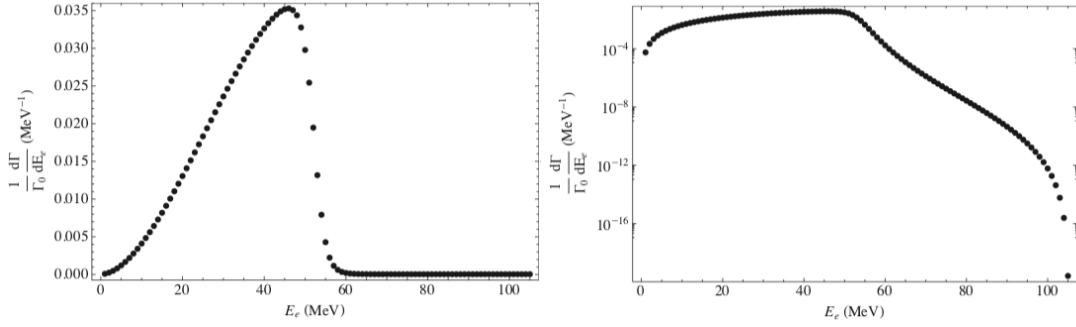


Figure 4: Spectrum of the DIO background, on normal scale on the left, on logarithmic scale on the right. It is possible to notice the presence of events in the signal region.

The spectrum shape drove also the requirement for detector momentum resolution. In the signal region (~ 105 MeV) the background has an intensity that is $\sim 10^{-17}$. With a bad resolution, spectra will be broader. This will bring a greater contribution of DIO background in the signal region, hence to a worse separation between signal and background. So, from simulation, it was seen that the resolution required to reach the declared single event sensitivity is near 180 keV. This led to the choice for the low mass straw chamber.

Other backgrounds are present, but they are less important than DIOs for the discussed topic, so they will be explained briefly.

Some backgrounds are related to the beam and its production. The most important is the one caused by the Radiative Pion Capture (RPC). RPC is a process that occurs when a pion is in a bound state with a nucleus and is captured by it, emitting a photon. The photon can convert in a nuclear field, yielding a e^+e^- pair, or undergo on a Compton scattering, releasing a single electron. In case of an asymmetric conversion the electron, or the positron, can have a momentum near the signal region.

This background drove the beam structure design: reactions caused by pions occur in a shorter time than ones by muons, about 200 ns and 800 ns respectively after the arrive of the beam. Using a pulsed beam, with a period of 1695 ns, and measuring the outgoing particles only after 700 ns one avoids to measure most of the particles coming from the pion reactions, and to search for conversion electrons in a cleaner environment.

Another background is the one caused by cosmic rays, in particular this is

largest background in the experiment.

Cosmic rays can produce electrons indistinguishable from signal electrons, hitting the stopping target or decaying near the detector and yielding an electron with an energy equal to E_e . From simulations the experiment expects ~ 1000 events like these, that means Mu2e requires a cosmic ray veto with an efficiency near 99.99%. It was already designed as explained before.

2.4 Lepton Number Violation search

With the Mu2e apparatus it will be possible to perform also other searches, in addition to muon to electron conversion, thanks to the detector's charge symmetry. One of these is the search for muon to positron conversion:

$$\mu^- + (A, Z) \rightarrow e^+ + (A, Z - 2)$$

This is an example of Lepton Number Violating (LNV) process, with a difference $|\Delta L| = 2$ between initial and final state, where L is the lepton number.

In this process the signal is similar to the one for the muon to electron conversion; there is a single positron emitted from the stopping target, with an energy of:

$$E_e = m_\mu - B_\mu - E_{N,rec} - \Delta_{Z-2}$$

Here the Δ_{Z-2} is the difference between initial and final nuclear binding energy.

A big difference between this process and muon to electron conversion process is that here the initial and final nuclear state are different. This means also that the nucleus at the end of the process can stay in two different states: ground state or excited state.

In the first case the energy is monochromatic, around 92 MeV. So the discussion gave previously for muon to electron conversion applies also in this case, unless for a bigger overlap between backgrounds and signal, due to the smaller energy of emitted particle.

In the case of the transition to excited state there is the possibility that the nucleus in the final state can occur in to a Giant Dipole Resonance (GDR). In that case the energy is no longer monochromatic, but the spectrum of emitted positrons has a width of about 20 MeV.

More informations about $\mu^- + (A, Z) \rightarrow e^+ + (A, Z - 2)$ and experimental searches of it can be found in [1].

3 Radiative Muon Capture

One of the beam related backgrounds is the one caused by Radiative Muon Capture. The spectrum of this process in the case of the $\mu^- \rightarrow e^-$ search does not reach the signal region, but it can overlap and distort the spectrum of other backgrounds, so its study is needed. It can not be said the same for the $\mu^- \rightarrow e^+$ search, where it can overlap the LNV signal region.

Radiative muon capture is a process that occurs when a muon is in a bound state with a nucleus and interacts with it. During the process a neutrino and a photon are produced. It differs from the ordinary muon capture, where no photons are emitted.

The process is:

$$\mu^- + (A, Z) \rightarrow \nu_\mu + \gamma + (A, Z - 1)$$

Also here, as in the RPC process, the emitted photons can convert and yield e^+e^- pairs. The spectrum of electrons and positrons given by this process has a range in aluminum that causes an overlap with spectra of backgrounds and signals interesting for the experiment.

Because of this, it is necessary to know the shape and intensity of the RMC spectrum as well as possible in the momentum range interesting for the Mu2e experiment, hence between 80 MeV and 105 MeV, in order to understand the relative intensity of various processes and to predict correctly the overall spectrum.

For muon to electron conversion the RMCs spectrum does not overlap directly with the $\mu^- \rightarrow e^-$ signal, because RMCs in aluminum have a kinematic endpoint in their momentum spectrum that is smaller than the value of the signal (it will be discussed later).

But there is an important overlap with the DIOs background spectrum, which should be taken in account for the subsequent reason. For DIOs there exists a good theoretical prediction, that describes spectrum of electrons emitted during this process. This prediction will be used to fit experimental data after data acquisition in a region with high statistics at lower momentum than the signal region. Doing this one can extrapolate the number of electrons coming from DIO processes in the signal region. If one neglects RMCs in the spectrum region where the fit is performed, and in reality they are not negligible, the result of the extrapolation for the number of electrons will be affected by systematic uncertainties, or even worse, there will be a wrong prediction.

The RMC spectrum disturbs also the search for the muon to positron conversion, in fact here it overlaps with the LNV signal spectrum.

The purpose of this study is to obtain a spectrum for electron and positron that comes from RMCs that can be quantitatively compared to other spectra of signals and backgrounds. It is not possible to use only a theoretical prediction because it is not precise enough, as will be explained later, because of approximations made in order to calculate the spectrum. Experimental data provides additional information, but there is no dataset with statistics high enough for Mu2e purposes. Also this can not be used alone to predict spectrum.

Given this, it was chosen to perform Monte Carlo simulations to obtain spectra for electrons and positrons coming from RMCs in the Mu2e experiment.

3.1 Theoretical description of RMC

One of the difficulties connected to the study of this process is the fact that no good enough theoretical model for RMC exists so far, as already said. It is possible to calculate a prediction for the momentum spectrum of emitted photons, but only using some approximations.

The model that is usually used studying the RMC process is the one that comes from the closure approximation. The difficulties of the theoretical description come from the multiple final states that the nucleus can assume after the interaction, and how they should be taken in account. In the closure approximation the momentum of the nucleus in the final state is averaged and a single value is considered in the calculations.

The closure approximation predicts a shape for the photon spectrum that is:

$$\frac{d\Lambda_\gamma(E_\gamma)}{dE_\gamma} \propto (1 - 2x + 2x^2)x(1 - x)^2 \quad (1)$$

Where E_γ is the energy of the photon and $x = E_\gamma/k_{max}$. The shape of the spectrum can be seen in Figure 5.

k_{max} is the only parameter that describes the spectrum, it is the maximum momentum of the emitted photons.

The value of k_{max} is not predicted by the theory, and only some guesses can be made about its value.

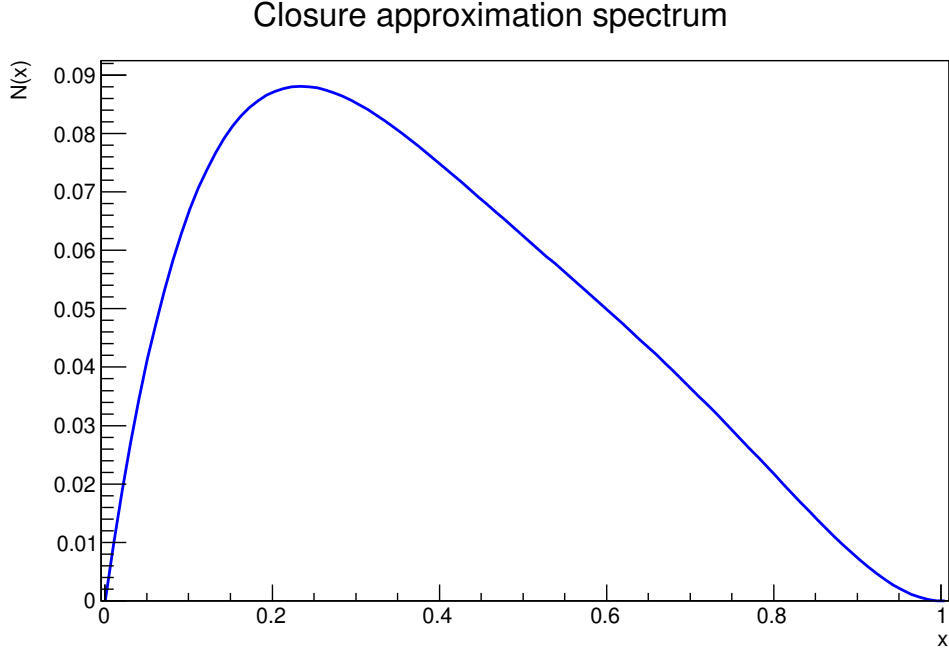


Figure 5: RMC photon spectrum predicted by the closure approximation.

The first guess for the value of k_{max} is the maximum momentum permitted by the kinematics of the process. In aluminum it takes the value:

$$E_{RMC}^{end} = m_{\mu} + M(A, Z) - M(A, Z - 1) - B_{\mu} - E_{rec} = 101.853 \text{ MeV}$$

Where m_{μ} is the muon mass, $M(A, Z)$ is the mass of the nucleus in the initial state, $M(A, Z - 1)$ is the mass of the nucleus in the final state, B_{μ} is the binding energy of the muon in the bound state with the nucleus and E_{rec} is the recoil energy of the nucleus.

Another guess for the value of k_{max} comes from the fit of data. When measured spectrum is fitted using the one from the closure approximation, a value for k_{max} can be extracted from data. This value is usually different from the kinematic one, smaller by about 10 MeV.

If the values of k_{max} for the two guesses are different, both of them can be used in this study to perform simulations, for reasons explained in the next section.

3.2 Previous measurements

Armstrong *et al.* [2] measured spectrum of photons emitted during RMC in various materials, including also aluminum, the material we are interested in.

The plot obtained from this measurement is shown in Figure 6.

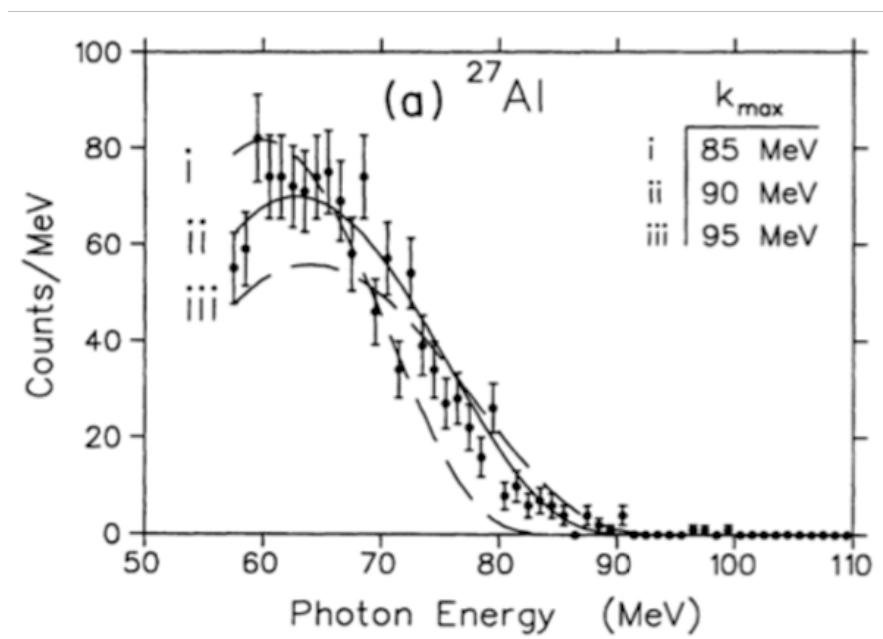


Figure 6: Spectrum of the photons emitted during RMC processes in aluminum; also three different fits are shown in figure.

As can be seen from the uncertainties in the spectrum and in the extracted values, this measurement has not collected enough statistics to permit the use of the measured spectrum for Mu2e's purposes. The measurement provides important information on the RMC photon spectrum, that can be used together with the theoretical predictions during simulations.

Here the value of k_{max} that best describes the data is extracted, fitting data with the closure approximation spectrum. It gives $k_{max} = 90 \pm 2$ MeV. As revealed in advance it is smaller than the kinematic endpoint by about 10 MeV.

In principle this value should be used to simulate dataset, instead of the other one, seeing that it that comes from experimental measurement. But in reality this is not obvious. Looking more in detail the Figure 6 in the region near 100 MeV, it can be seen that the number of events is different from zero in

some bins, near the kinematic endpoint of the process. The statistics collected in the measurement is not sufficient to discriminate whether this is a tail due to the RMCs photon emission, or if it is only a casual contribution.

So both of the guesses remain plausible as description for the process, and both of them will be used to perform simulations.

Armstrong *et al.* measured also another quantity during the experiment: the fraction of photons with a momentum greater than 57 MeV respect to the total number of muon captures (ratio expressed here as $R_\gamma(E > 57 \text{ MeV})$).

The measured value is:

$$R_\gamma(E > 57 \text{ MeV}) = (1.43 \pm 0.13) \cdot 10^{-5}$$

Also a theoretical prediction for that quantity is provided in [2]. It is expressed by:

$$R_\gamma = \left(\frac{e^2}{\pi}\right) \left(\frac{k_{max}^2}{m_\mu^2}\right) (1 - \alpha) \int_{E_{min}/k_{max}}^1 (1 - 2x + 2x^2) \cdot x \cdot (1 - x)^2 dx \quad (2)$$

The prediction for R_γ depends on k_{max} , from the evaluation of the integral and directly as k_{max}^2 .

The dependence can be seen in Figure 7.

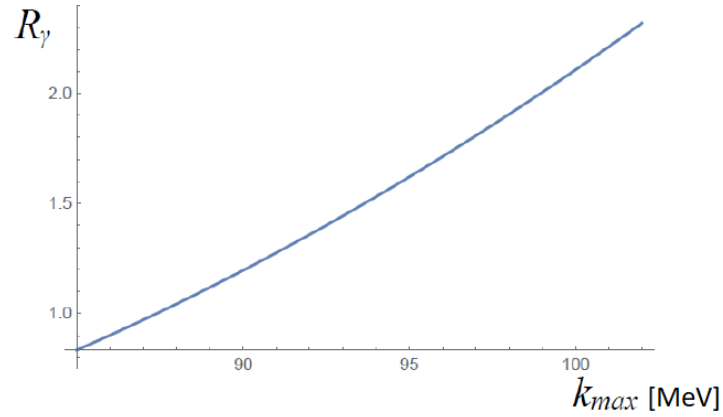


Figure 7: Plot shows the values of R_γ in function of k_{max} .

It can be noticed from Figure 7 that using the extracted value of k_{max} of 90 MeV in (2) the calculated value for R_γ does not match with the experimental

measurement. Indeed to obtain a value of R_γ equal to the measured one, the k_{max} that has to be used is ~ 93 MeV. This shows again that the theoretical prediction describes only roughly spectrum and its shape.

For the preceding reasons, if one wants to use different values for k_{max} , the predicted value for R_γ will be different from the measured one, but one wants to avoid this and harness experimental data.

This is taken in account while performing simulations, in particular modifying the normalization and the shape of spectra used to generate samples.

Momenta are generated extracting random values from a uniform distribution in a predefined range. Only after that, every event is weighted with the corresponding value of the spectrum at the extracted momentum. This provides the same number of events in all the region, hence the same statistics.

Here the spectrum used to weight events is the spectrum coming from closure approximation in the range between 80 MeV and the k_{max} used in each simulation. However the spectrum is modified, in order to match the experimental information, forcing R_γ to be equal to $1.43 \cdot 10^{-5}$ for each value of k_{max} , instead of the value predicted from theory using equation (2), in principle different from the measured one.

This is done with the applied weight, that does not consider only the value of spectrum at that momentum, but is composed also of other terms, that will be explained soon.

Together with this, the weight used takes in account the fact that the simulation is performed in a different range of momentum than the one considered in the measurement done by Armstrong *et al.*, hence from 80 MeV instead of 57 MeV.

The value of the weight used for the histograms is:

$$W = 1.43 \cdot 10^{-5} \cdot \frac{R_\gamma(> 80 \text{ MeV})}{R_\gamma(> 57 \text{ MeV})} \quad (3)$$

The use of this kind of weight normalization modifies the spectrum shape in a way that can be seen in Figure 8.

Doing this one can use different guesses for k_{max} in simulations, seen that because of the statistics is not clear which vale of k_{max} describes better the process, but maintaining the experimental information about the fraction of photons in the normalization.

Spectra at the bottom of Figure 8 are used to generate samples.

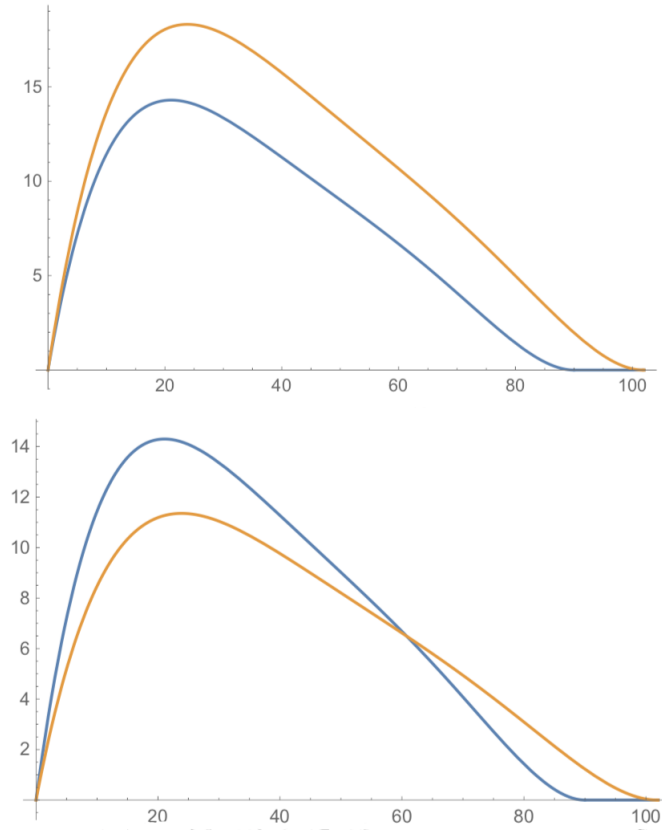


Figure 8: Spectra from closure approximation. At the top of the figure spectra are shown when only weight from closure spectrum is applied, at the bottom of the figure spectra when the weight W is applied.

4 Data samples

Theoretical prediction and previous measurement of RMC photon spectrum will be used as basis for the simulation, but for the explained reasons they can not be used alone as a prediction. Generation of data samples through Monte Carlo simulations is necessary in order to obtain a prediction with sufficient high statistics for Mu2e needs.

Simulations are performed through grid run, using Mu2e machines. Four different samples are generated:

- RMC photons with $k_{max} = 90$ MeV
- RMC photons with $k_{max} = 95$ MeV

- RMC photons with $k_{max} = 101.853$ MeV
- DIO with minimum momentum of 70 MeV

In the RMCs samples photons are generated, with a momentum between 80 MeV and the relative k_{max} . The spectrum does not start before that value because there is almost zero acceptance of the experiment given by the annular geometry.

The spectrum used is the one given by the closure approximation, but modified as explained in the previous section to match the experimental data for every value of k_{max} . This strategy is used in order to harness all information that are known so far, both theoretical and experimental.

The photons can go into an internal ¹ or an external conversion. In both of them the photon interacts with a nucleus, yielding a e^-e^+ pair: in the first case the interaction is with the same nucleus that captured the muon, while in the second one the nucleus that converts the photon is another one in the apparatus.

The photons can go also into a Compton scattering, where a single electron is emitted in the process. This will cause an asymmetry between entries in the histograms of electrons and positrons, bigger in the first one.

In the DIOs sample electrons are generated ² with a momentum between 70 MeV and the endpoint. This sample starts 10 MeV before the others because there are negligible number of electrons before 70 MeV.

The spectrum used to generate these events is the one shown in Figure 4.

After that, e^-e^+ produced are reconstructed by the simulation of the Mu2e apparatus and the reconstructed tracks are stored into standard Mu2e ntuples, that are analyzed through a Root macro in order to produce histograms.

4.1 Normalization of histograms

The principal purpose of this study is to compare RMC spectra with different k_{max} with each other and with DIOs background spectrum.

In order to do this is necessary to normalize all histograms coherently. Here we arbitrary chose to normalize all histograms to the expected number to be seen in the experiment.

¹The fraction that goes into internal conversion is the 0.69 % of the total.

²Positrons are not generated because the beam consists only of negative muons.

To normalize RMC spectra to the total life experiment one has to multiply by:

- the total number of protons that will be used in the experiment;
- the number of muons that stop for every incident proton;
- the fraction of stopped muons of the total that are captured by the nucleus;
- the number of RMCs with a momentum in the range where the simulation was performed for every muon capture.

Doing this one obtains the total number of the RMC processes in the range of acceptance of the Mu2e apparatus ³ during all the data acquisition.

The resulting factor F for RMCs is:

$$F = \frac{\#protons}{experiment} \cdot \frac{\#stopped \mu}{proton} \cdot \frac{\#captured \mu}{\#stopped \mu} \cdot W \quad (4)$$

Where:

$$\frac{\#protons}{experiment} = 3.6 \cdot 10^{20} \quad \frac{\#stopped \mu}{proton} = 0.0019 \quad \frac{\#captured \mu}{\#stopped \mu} = 0.6067$$

And W assumes different values for every value of k_{max} , it depends in fact by the range of momentum used to normalize histograms:

- $W_{>90MeV} = 6.92 \cdot 10^{-7}$
- $W_{>95MeV} = 1.47 \cdot 10^{-6}$
- $W_{>102MeV} = 2.65 \cdot 10^{-6}$

The DIO spectrum is normalized with the same strategy, the only difference is that the last two factors in (4) are replaced by the fraction of muons that decay in orbit normalized to the number of stopped muons.

That factor values:

$$\frac{\#DIO}{\#stopped \mu} = 0.3933$$

N.B. The number of generated events is applied every time as an external factor, that divides the histogram.

³Hence that will be measured.

4.2 Spectrum histograms

Data samples generated are analyzed with a Root macro. It takes events from a tree and fills the histogram with the value of reconstructed momentum of e^- (or e^+) for each event in the tree, applying also the weight W already discussed.

Not all reconstructed events are used to fill histograms, some cuts are applied. The applied ones are the standard reconstruction cuts for Mu2e.

A different histogram for e^- and e^+ is produced for every sample of RMC photons, and only e^- histogram is obtained from the DIO sample.

Obtained histograms can be found in Figure 11, 12, 13 and 14 in the Appendix.

For RMC histograms same comments can be made for every e^- histogram and e^+ histogram.

The first thing that can be noticed is that as expected the maximum momentum of particles is near the k_{max} used in every sample. In reality it is a little lower. This is due to the kinematics of the conversion process: the phase space available for the production of an e^\pm of a certain momentum decreases when the value of the e^\pm momentum is close to the momentum of the photon that is yielding the pair. In the region near k_{max} can be present only e^\pm that has to take all photon momentum. Hence the probability to produce an e^\pm in that region is smaller than in regions of lower momentum, where e^\pm can come also from the conversion of photons with higher momentum. When the statistics of the simulation is not enough high, the region at high momentum can be empty, as in this case.

Some comments can be made on the shape of histograms; this is given by the convolution of the spectrum used to generate data with the detector response. On right side of spectra, the one at higher momentum, the shape is given mainly by the spectrum used to generate the sample, i.e. the "modified" closure spectrum. This trend, as can be seen in all histograms, does not continue up to momenta lower than ~ 80 MeV. At this point in fact the acceptance given by annular geometry of the apparatus plays a significant role and restricts strongly the number of reconstructed particles, causing the visible sharp cut.

This can be seen in all the presented spectra, and as confirmation of that already said, it can be noticed that the fall due to the acceptance remains stable in momentum, while the maximum momentum of particle increases, causing a

larger spectrum for samples generated with greater value of k_{max} .

Looking at the number of entries of histograms can be seen that the ones for e^- are always larger than the ones for e^+ . This is right and expected as already said, because positrons can be produced only in e^-e^+ pairs, single electrons can be released in a Compton scattering. So the excess of e^- is due to the presence of these two different processes.

For the histogram showing the spectrum of DIO sample, present in Figure 11, comments similar to previous can be made. Also here the overall shape is given by the simultaneous contribution of the spectrum used to generate events and of the acceptance of the apparatus. As already said, here only the e^- histogram is present, for the composition of the muon beam.

5 Comparison between spectra

Once that histograms are produced, and they are normalized coherently to the total life of the experiment, they can be correctly compared, in order to understand the relative intensity and the possible overlaps between processes.

Using e^- histograms we can perform a quantitative comparison between RMC and DIO spectra, that will provide a useful information for the experiment development, in addition to a comparison between RMC spectra with different values for k_{max} .

Using e^+ histograms one can extract information about the differences between RMC spectra with different values for k_{max} .

5.1 e^- spectra comparison

The histogram obtained by the superposition of the four e^- spectra is shown in Figure 9.

Important information can be extracted from the study of this plot. The first thing is the difference between RMC spectra with different k_{max} . This difference is evident and can not be neglected in the analysis. In fact the use of different k_{max} modifies the maximum momentum of emitted particles as expected, but also the average number of the RMC event, since $R_\gamma \propto k_{max}$.

The most important information that can be extracted from this plot is given by the comparison of the relative intensity of RMCs and DIOs. In all considered

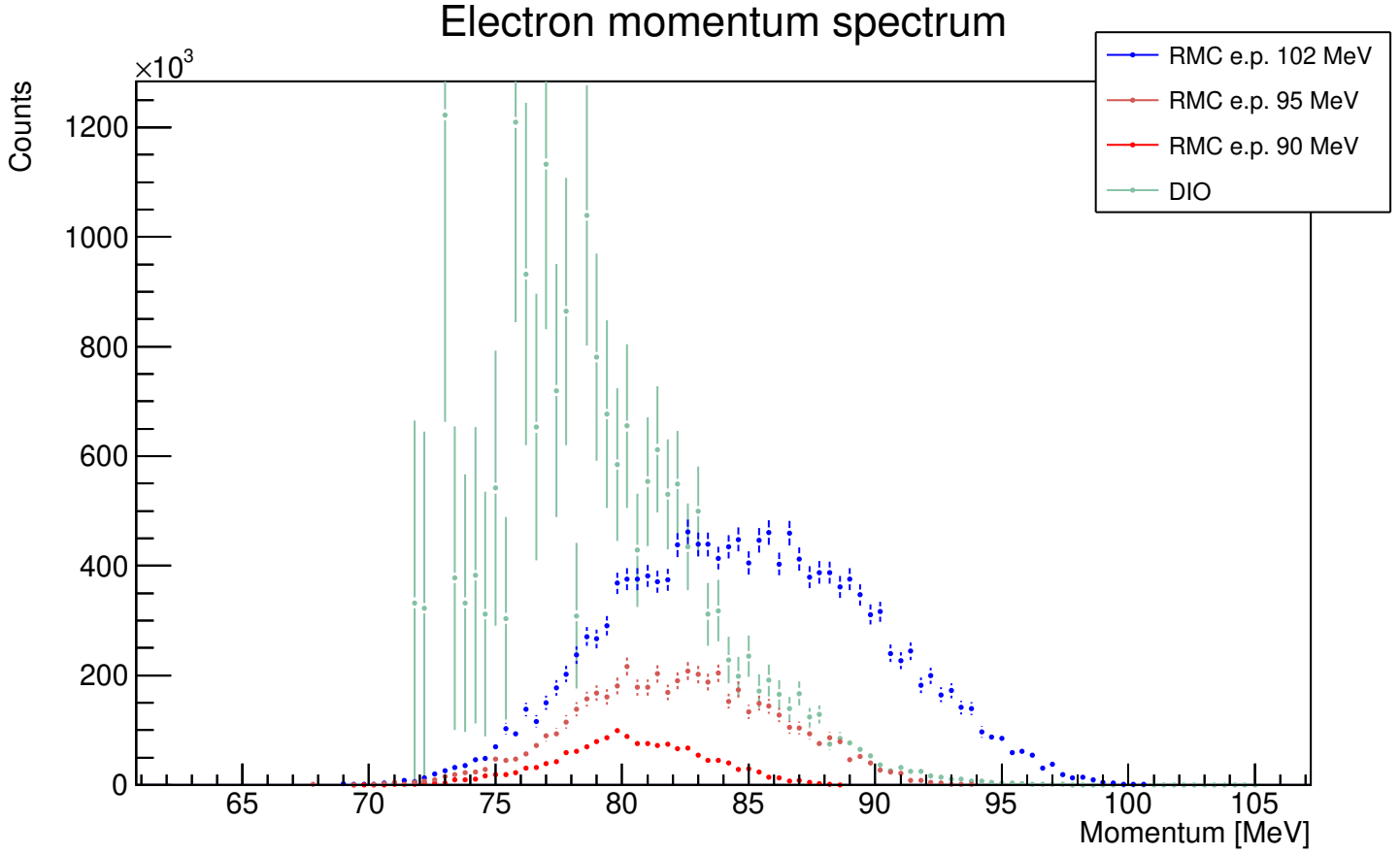


Figure 9: Histogram given by the superposition of spectra obtained from e^- generated samples.

cases, in particular also in the best fit from Armstrong *et al.* ⁴, the contribution given by the RMC signal to the overall spectrum is never negligible compared to the DIO contribution.

For example one can look at values of spectra near 80 MeV: here the RMCs spectrum is $\sim 10\%$ of the DIOs spectrum.

This means that RMCs have to be considered during the fit to the DIO spectrum in the high statistics region (lower momentum than signal region). If this is not done, one can obtain larger uncertainties, or worse, incorrect predictions for the DIO background contribution in the signal region.

⁴Where RMCs have the smallest intensity, with $k_{max} = 90$ MeV.

5.2 e^+ spectra comparison

The histogram obtained by the superposition of the three e^+ spectra is shown in Figure 10.

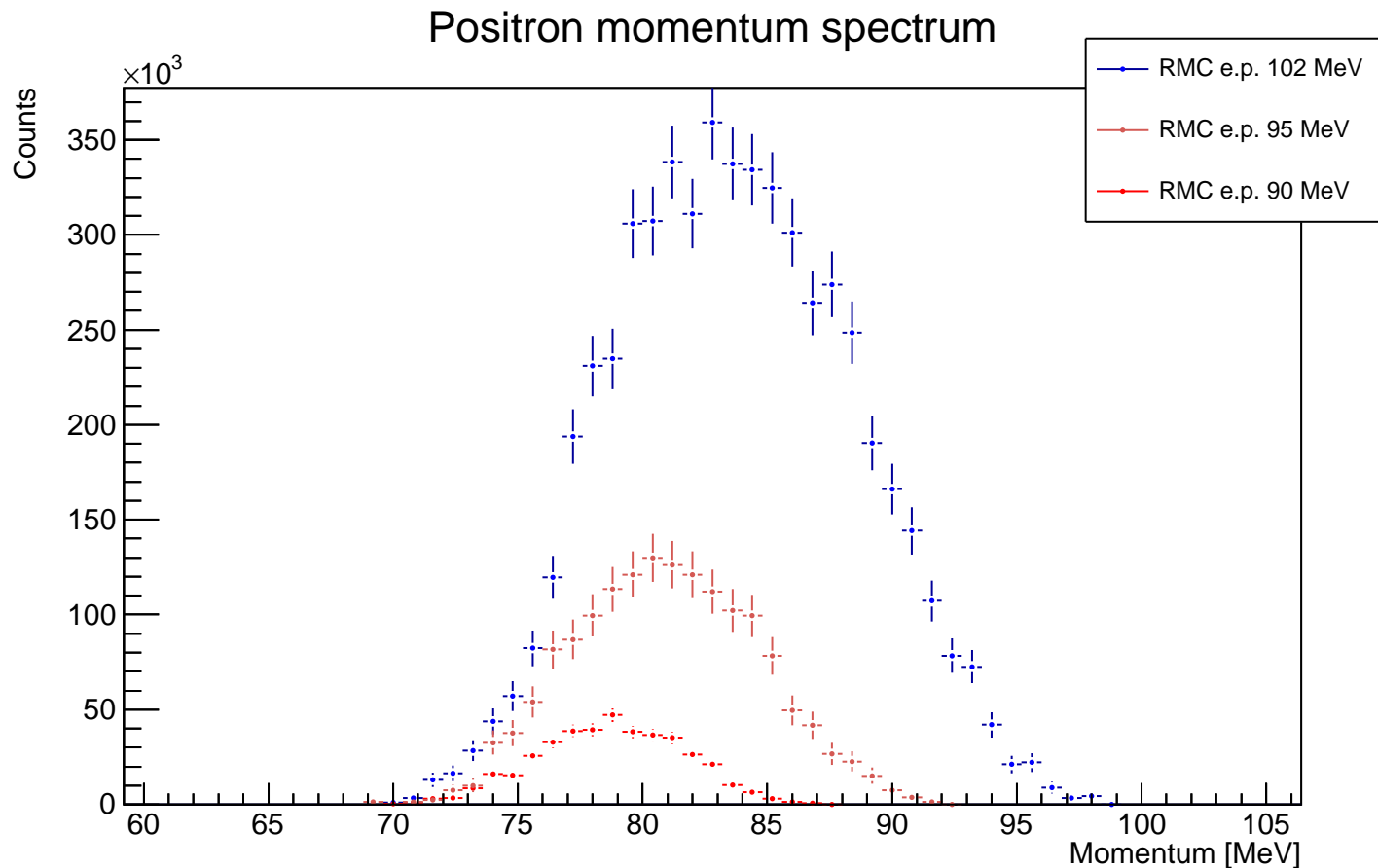


Figure 10: Histogram given by the superposition of momentum spectra obtained from e^+ generated samples.

Information similar to the previous plots can be extracted from this plot. We can also see here the non-negligible difference between spectra with different k_{max} , both in maximum momentum and number of events.

From here one can see also that k_{max} determines the overlap between RMC signal and the $\mu^- \rightarrow e^+$ conversion signal. In fact only for the spectrum with $k_{max} = 102$ MeV the $\mu^- \rightarrow e^+$ signal region is completely overlapped. In the case of $k_{max} = 95$ MeV is not clear if this signal region is affected by the RMC signal, more statistics should be added to determine that. In the case of $k_{max} = 90$ MeV

the spectrum given by RMC stops before the signal region.

6 Conclusions

With the simulations performed in this study, using information from previous measurements and theory, we studied the background given by the conversion of photons coming from RMC processes.

Comparing obtained RMC spectra with each other and with the one for DIO processes we find some information:

- the range and the intensity of the spectrum for e^\pm due to RMCs depends on the maximum momentum of the emitted photons;
- in the case of e^+ spectrum the region containing conversion signal is strongly overlapped with the RMC signal only in the case of $k_{max} = 102$ MeV;
- the spectrum of e^- given by RMC processes is never negligible compared to the spectrum of DIO processes; RMCs have to be considered in the analysis in order to not misunderstand overall spectrum shape.

7 Next steps

This work can be extended in some ways:

- more statistics can be added to simulations in order to obtain more detailed spectra;
- a different theoretical model for the RMC process can be provided, avoiding approximations, in order to obtain a better spectrum prediction, which can be used to simulate data samples and after to fit data, together with the DIOs theoretical prediction;
- the Radiative Pion Capture background spectrum can be added to this study, both in the e^+ and in the e^- spectrum, in order to compare intensity and shape with the obtained ones;
- Event Mixing background ⁵ spectrum can be added to the plot, in order to compare also the effect due to accidental events to already considered spectra.

⁵Accidental activity from the beam and particles produced in muon capture need to be included since they can contribute to dead time and lower the reconstruction efficiency.

8 Appendix

N.B. Histograms reported in the appendix does not have same number of bins, because of different number of entries on each histogram. This is due to number of generated events, that depends on the sample, mostly on the different acceptance of the reconstruction process, that decreases at momenta near 80 MeV.

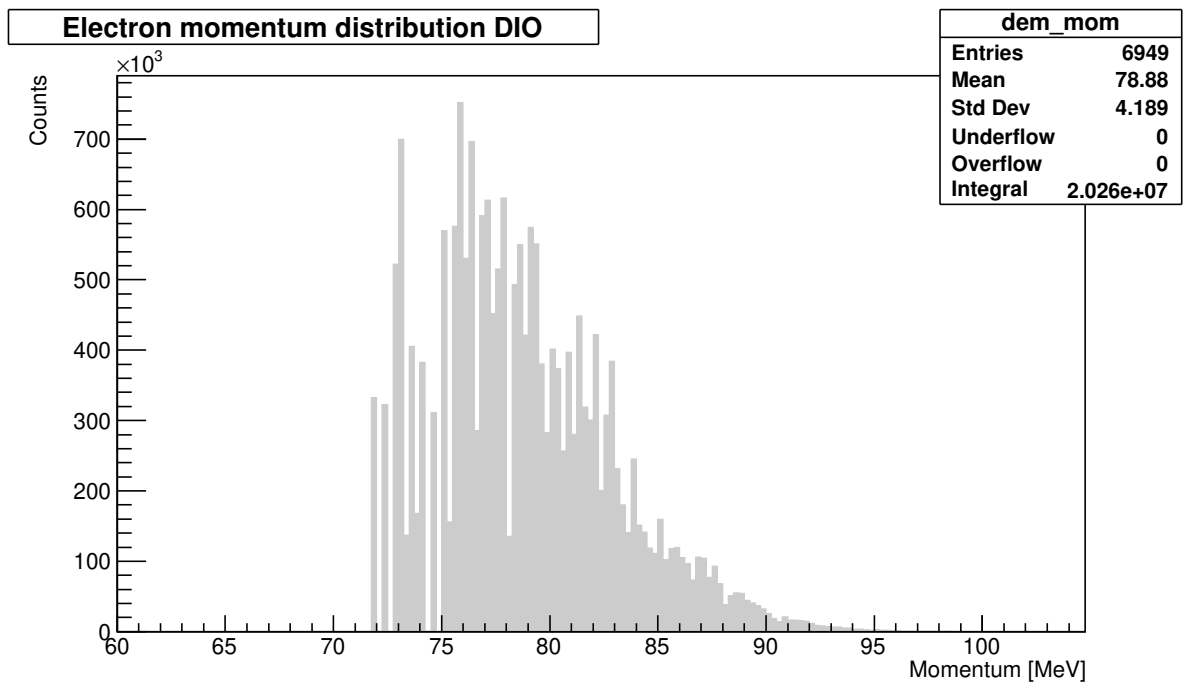


Figure 11: Histogram containing momentum spectrum for e^- , obtained from the DIO generated sample.

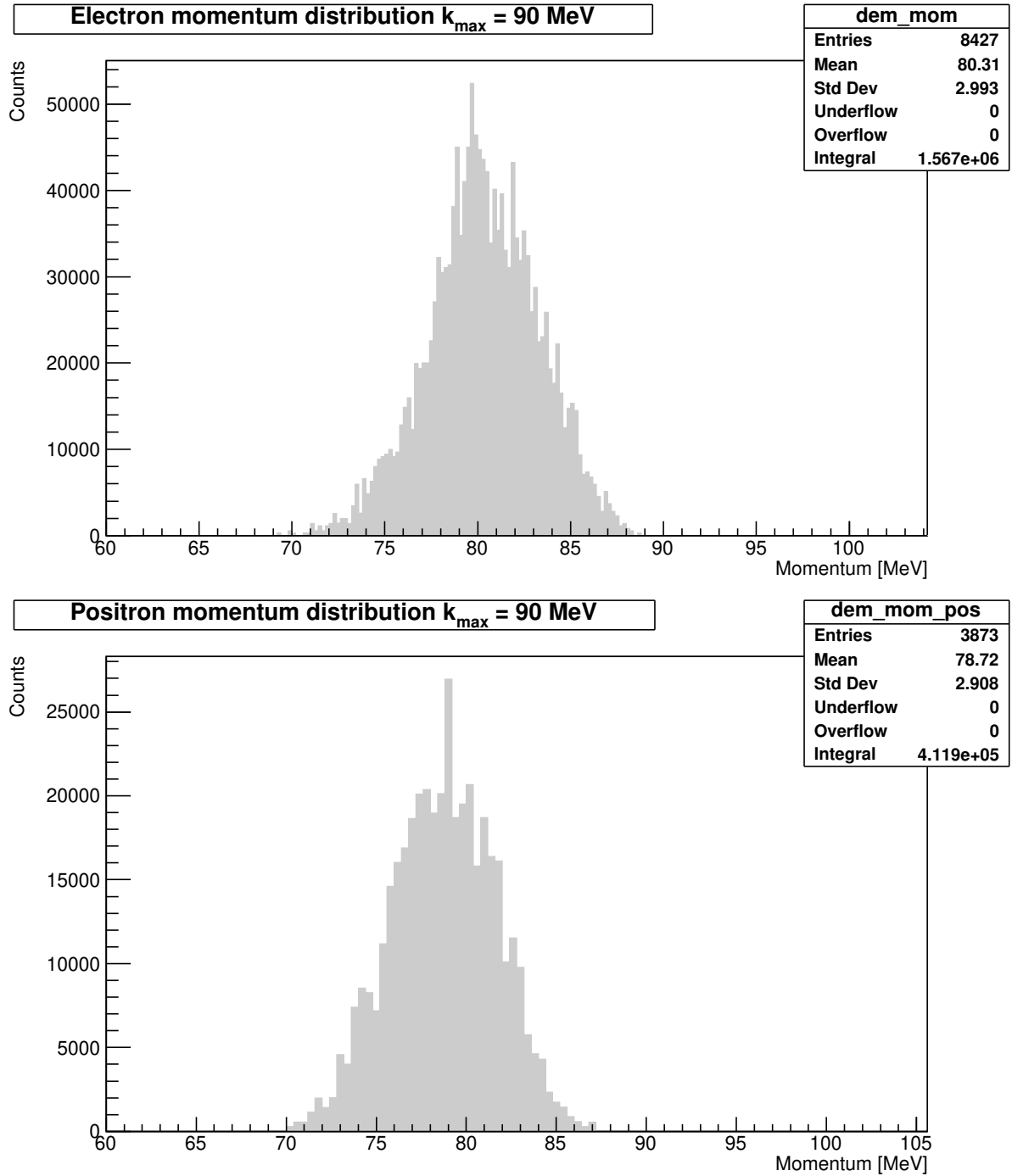


Figure 12: Histograms containing momentum spectra for e^- and e^+ , respectively on the top and the bottom of the figure, obtained from the RMC generated sample with a k_{max} of 90 MeV.

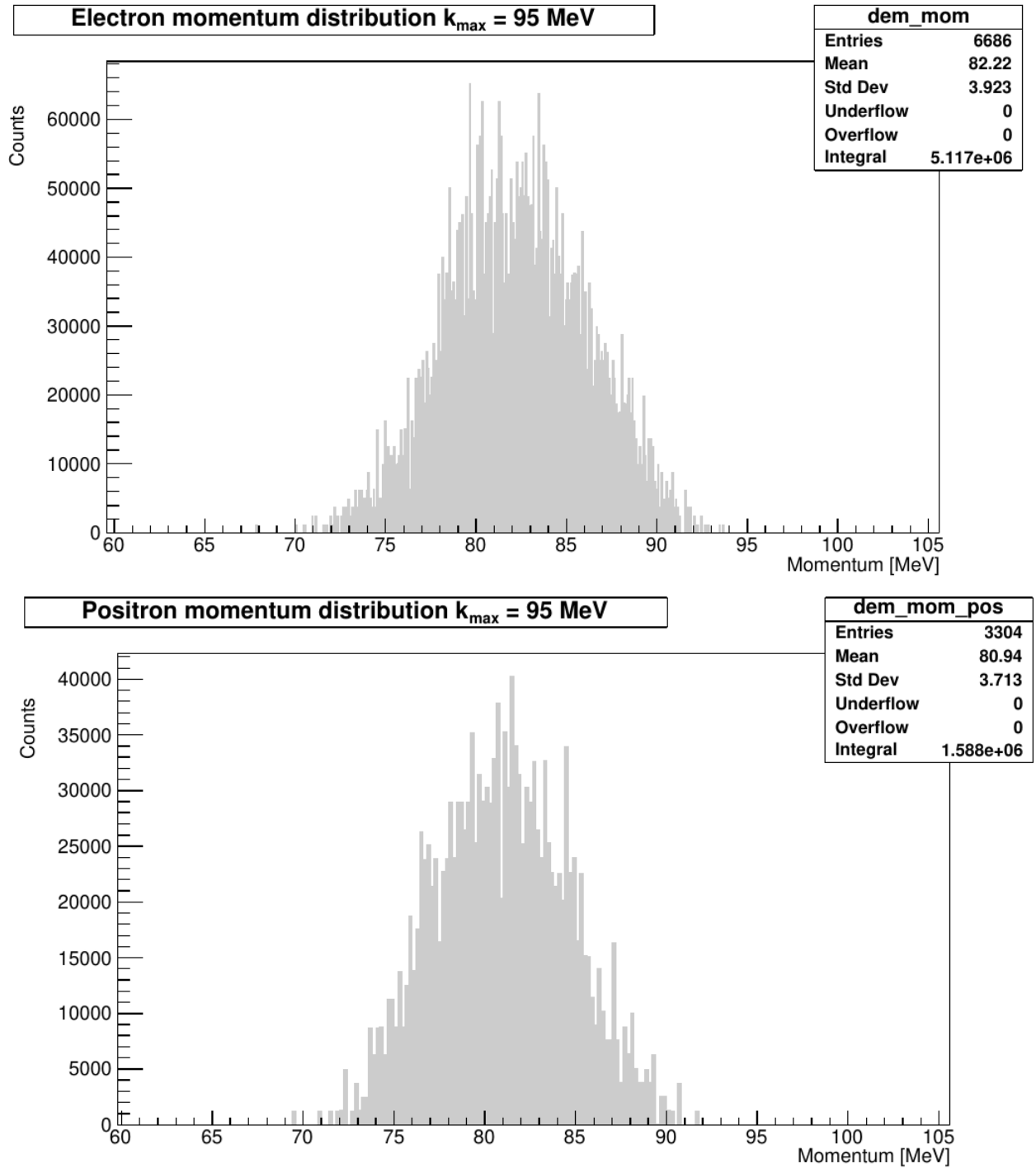


Figure 13: Histograms containing momentum spectra for e^- and e^+ , respectively on the top and the bottom of the figure, obtained from the RMC generated sample with a k_{max} of 95 MeV.

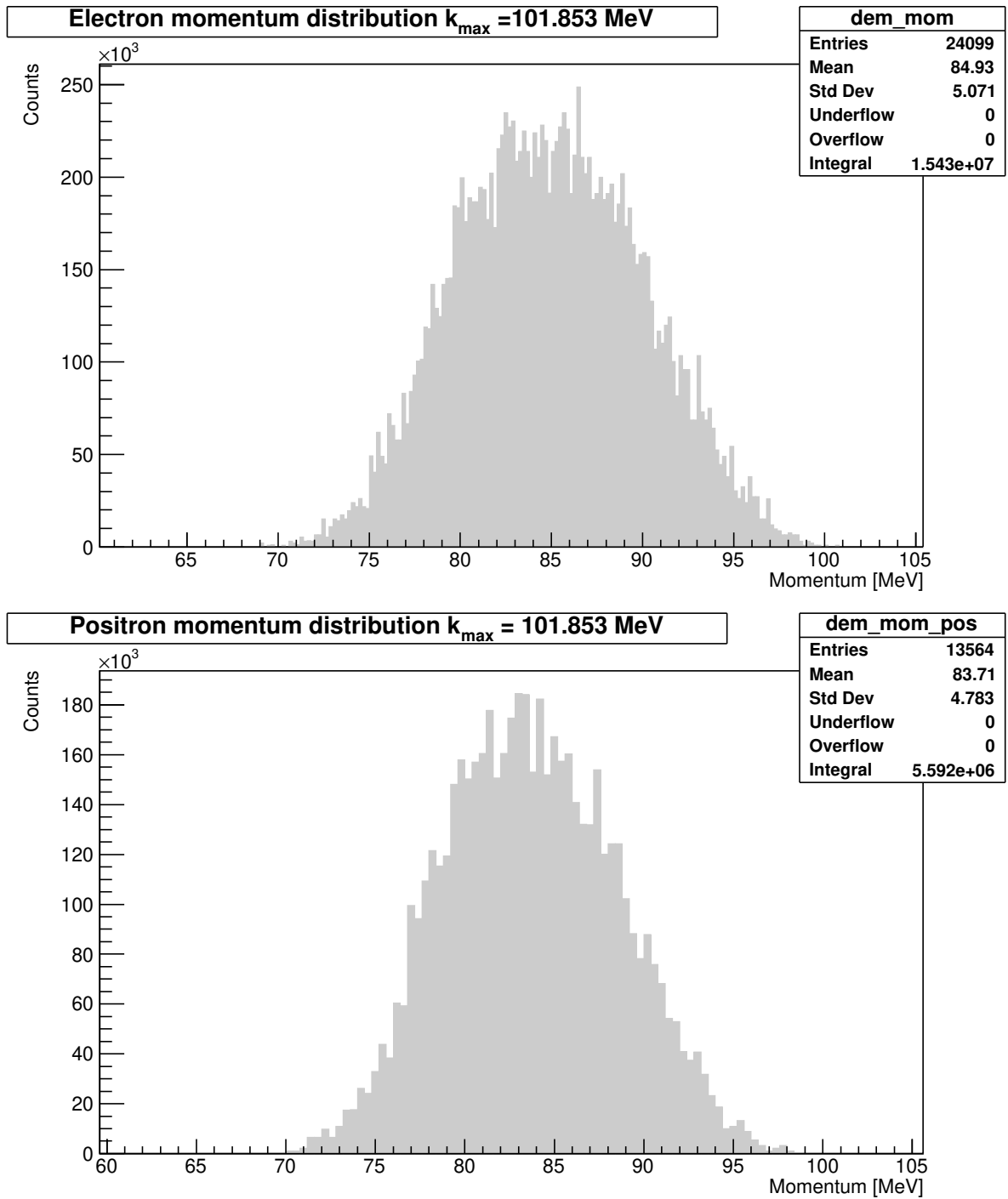


Figure 14: Histograms containing momentum spectra for e^- and e^+ , respectively on the top and the bottom of the figure, obtained from the RMC generated sample with a k_{max} of 101.853 MeV.

References

- [1] R. H. Bernstein & P. S. Cooper arxiv 1307.5787
- [2] R. Armstrong *et al.*, Phys. Rev. C **46**, 1094 (1992)
- [3] M. Gmitro and P. Truöl, Adv. Nucl. Phys. **18**, 241 (1987)
- [4] R. H. Bernstein mu2e-doc-db 18426.
- [5] P. Christillin, M. Rosa-Clot and S. Servadio, Ref. TH. **2697-CERN** (1979)